Supporting Information

Electrochemical Sensor-Adsorbent for Lead (Pb^{2+}) Ions in Aqueous Environment by Katiragum-Arginine Schiff Base

Rakesh Kumar Saren[1], Shankha Banerjee[2], Barun Mondal[1], Sanjib Senapati[2] and Tridib Tripathy[1*]

[1]Postgraduate Division of Chemistry, Midnapore College (Autonomous), Midnapore, PaschimMedinipur, 721101, West Bengal, India.

[2]Department of Biotechnology, BJM School of Bioscience, Indian Institute of Technology Madras, Chennai 600036, India.

[*]Corresponding author
E-mail:tridib.tripathy@midnaporecollege.ac.in, tridib_tripathy@yahoo.co.in
Tel/Fax: +913222275847

1. Experimental

1.1 Determination of dialdehyde content

The dialdehyde content in KGD is determined spectrophotometrically according to the previous report.[1] The detail procedure is given in our previous communication.[2] Shortly, a fixed amount of KGD is allowed to react with 2,4- dinitrophenyl hydrazine (2,4-DNPH) in water. The solution is vigorously stirred upto 90 min. The supernatant after centrifugation is analyzed by UV-VIS spectrophotometer (Schimadzu, Japan) at λ= 361 nm to estimate the unreacted DNPH. The dialdehyde content (DAC) in KGD is calculated by using the following equation

$$\mathrm{DAC(mmole/g)} = \frac{\text{Reacted 2,4-DNPH(mmol/g)}/198.14}{\text{Conc(\%)x}10^{-4}} \qquad \text{Eq. (S1)}$$

The dialdehyde content is found to be in the KGD 68.67 %.

1.2 Detection Limit

Following equation is used for the calculation of limit of detection (LOD).[3]

$$LOD = 3\sigma/\mathrm{K} \qquad \text{Eq. (S2)}$$

Where, σ is the standard deviation obtained from the graph of I (A) versus concentration of KGDR (Fig. S7b) and K refers to the slope of the calibration curve obtained by plotting current I (A) vs concentration of Pb^{2+} (Fig. 4b).

1.3 Adsorption Kinetics

Pseudo first order, pseudo second order kinetics and intra particle diffusion kinetic models are used to evaluate the adsorption kinetics.

The pseudo first order or Lagergren kinetic model is expressed by the following equation[4]

$$\ln(q_e - q_t) = lnq_e - k_1 t \qquad \text{Eq. (S3)}$$

where, q_e and q_t are the amount of Pb^{2+} adsorbed by KGDR at equilibrium and at the time t respectively in mg g^{-1}, k_1 is the pseudo first order rate constant which is calculated from the slope of the plot $\ln(q_e - q_t)$ versus t.

The pseudo second order kinetic model is expressed by the following equation[5]

$$\frac{t}{q_t} = \frac{1}{k_2 q_e^2} + \frac{1}{q_e} t \qquad \text{Eq. (S4)}$$

Where, k_2 is the pseudo second order rate constant in g mg^{-1} min^{-1} is calculated from the slope and intercept of the plot of t/q_t versus t.

The intra particle diffusion model is developed by Weber and Morris,[6] which explains the diffusion kinetics and mechanism of adsorption. It is represented as:

$$q_t = k_d t^{1/2} + c \qquad \text{Eq. (S5)}$$

Where, k_d ($mg.g^{-1}.min^{-1/2}$) is the intra particle diffusion rate constant, c is the boundary layer thickness. k_d and c are calculated from the slope and the intercept of the plot q_t versus $t^{1/2}$ respectively.

1.4 Adsorption isotherms

Three adsorption isotherm models namely Freundlich, Langmuir and Temkin are used to describe the adsorption equilibrium between the adsorbed [Pb^{2+}] and the residual [Pb^{2+}] in the solution over the entire studied concentration range.

Freundlich isotherm model is used to express the adsorption process onto the heterogeneous surface of the adsorbents. The isotherm is expressed by[7]

$$q_e = K_F C_e^{1/n} \quad \text{Eq. (S6)}$$

The linearized form of the adsorption is expressed by the following equation

$$lnq_e = lnK_F + \frac{1}{n} lnC_e \quad \text{Eq. (S7)}$$

Where, K_F ($L.g^{-1}$) and 1/n are Freundlich adsorption isotherm constants respectively. K_F and 1/n are calculated from the slope and intercept of the straight line plot lnq_e versus lnC_e.

In the Langmuir isotherm model, it is assumed that adsorption process takes place at the homogeneous sites of adsorbent's surface which is filled with non-interacting adsorbent molecules and the adsorption process follows monolayer adsorption mechanism. The linear form of the equation is expressed by[8]

$$\frac{1}{q_e} = \frac{1}{bq_m C_e} + \frac{1}{q_m} \quad \text{Eq. (S8)}$$

Where C_e ($mg.L^{-1}$) represents the equilibrium Pb^{2+} ion concentration, q_e ($mg.g^{-1}$) denotes amount of Pb^{2+} adsorbed onto the KGDR at equilibrium. q_m ($mg.g^{-1}$) and b ($L.mg^{-1}$) are Langmuir constants, which are calculated from the slope and intercept of the linear plot of $1/q_e$ versus $1/C_e$.

The characteristic parameter of Langmuir isotherm is expressed by a dimensionless parameter R_L, called equilibrium parameter which is represented as follows

$$R_L = \frac{1}{1+ bC_0} \quad \text{Eq. (S9)}$$

The R_L value lies within 0 to 1 indicate a favourable adsorption process.

Temkin isotherm model consider the adsorbent-adsorbate interaction where it is assumed that, increasing the surface coverage by adsorption linearly decreases the heat of adsorption of all the molecules in the layer. Temkin adsorption isotherm model is expressed by the following equation [9]

$$q_e = \frac{RT}{b_T} lnA_T + \frac{RT}{b_T} lnC_e \quad \text{Eq. (S10)}$$

Where A_T is the Temkin isotherm constant ($L.g^{-1}$), T is the absolute temperature, R is the universal gas constant and b_T is the Temkin constant related to the heat of adsorption B ($J.mole^{-1}$) [$B= RT/b_T$]. The value of A_T and b_T are calculated from slope and intercept of the plot q_e versus ln C_e.

1.5 Adsorption thermodynamics

Van't Hoff equation[10] is used to calculate various thermodynamic parameters like the enthalpy change (ΔH˚), changes in entropy (ΔS˚) of the adsorption in the temperature range 10˚C to 60˚C. The Van't Hoff equation is

$$lnK_T = \frac{\Delta S^\circ}{R} - \frac{\Delta H^\circ}{RT} \quad \text{Eq. (S11)}$$

The standard free energy (ΔG°) is calculated by the following equation

$$\Delta G^{\circ} = \Delta H^{\circ} - T\Delta S^{\circ} \quad \text{Eq. (S12)}$$

R is the universal gas constant (8.314 J.mol-1.K-1). The ΔH° and ΔS° are calculated from the linear plot between $\ln K_T$ versus 1/T. K_T is the thermodynamic equilibrium constant which can be calculated by using following equation[11]

$$K_T = \frac{S_e}{C_0 - S_e} \quad \text{Eq. (S13)}$$

Where S_e is the concentration of Pb^{2+} adsorbed onto KGDR at equilibrium and C_0 is the initial concentration of Pb^{2+}.

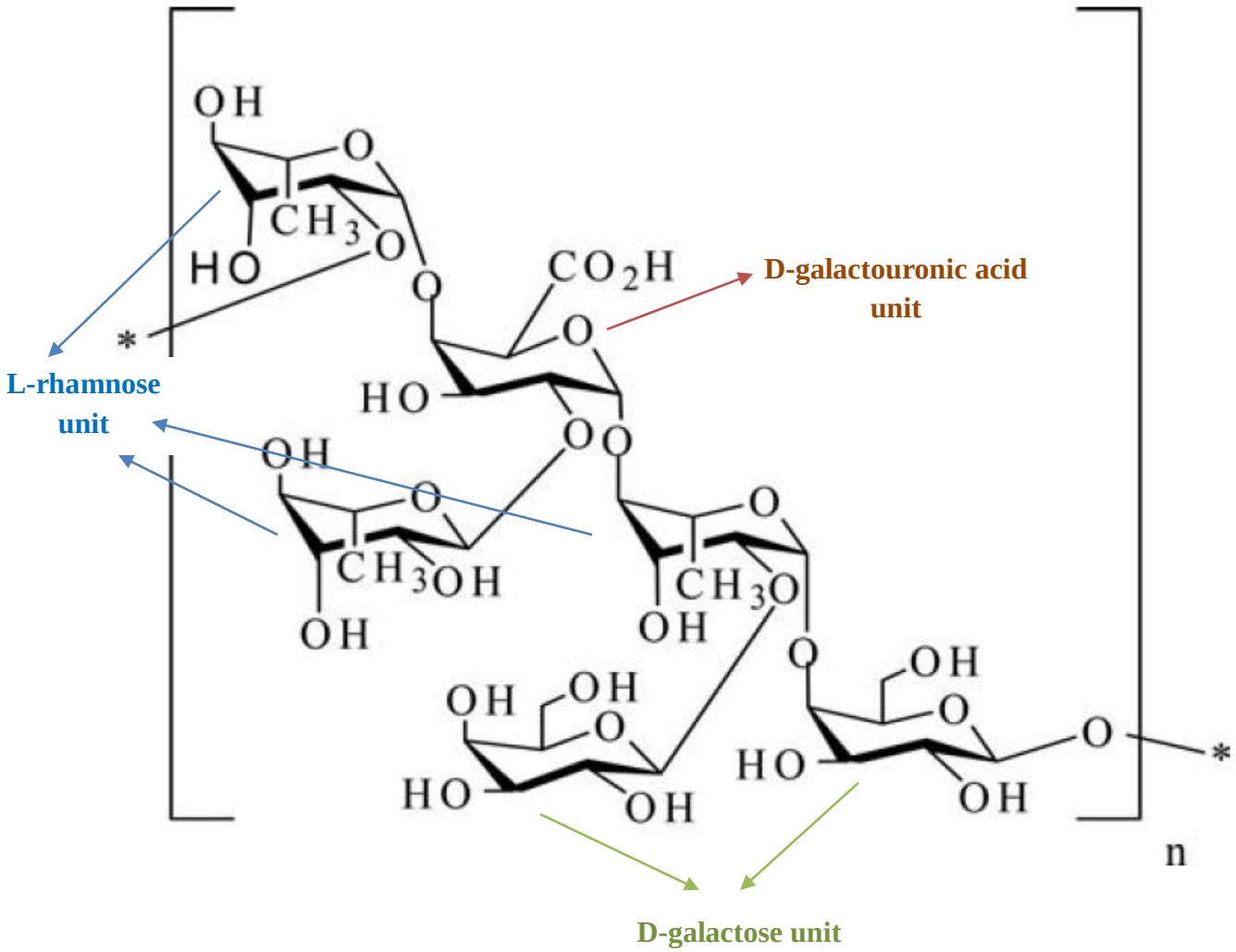

Fig. S1 The structure of Katiragum showing the monosaccharide units.

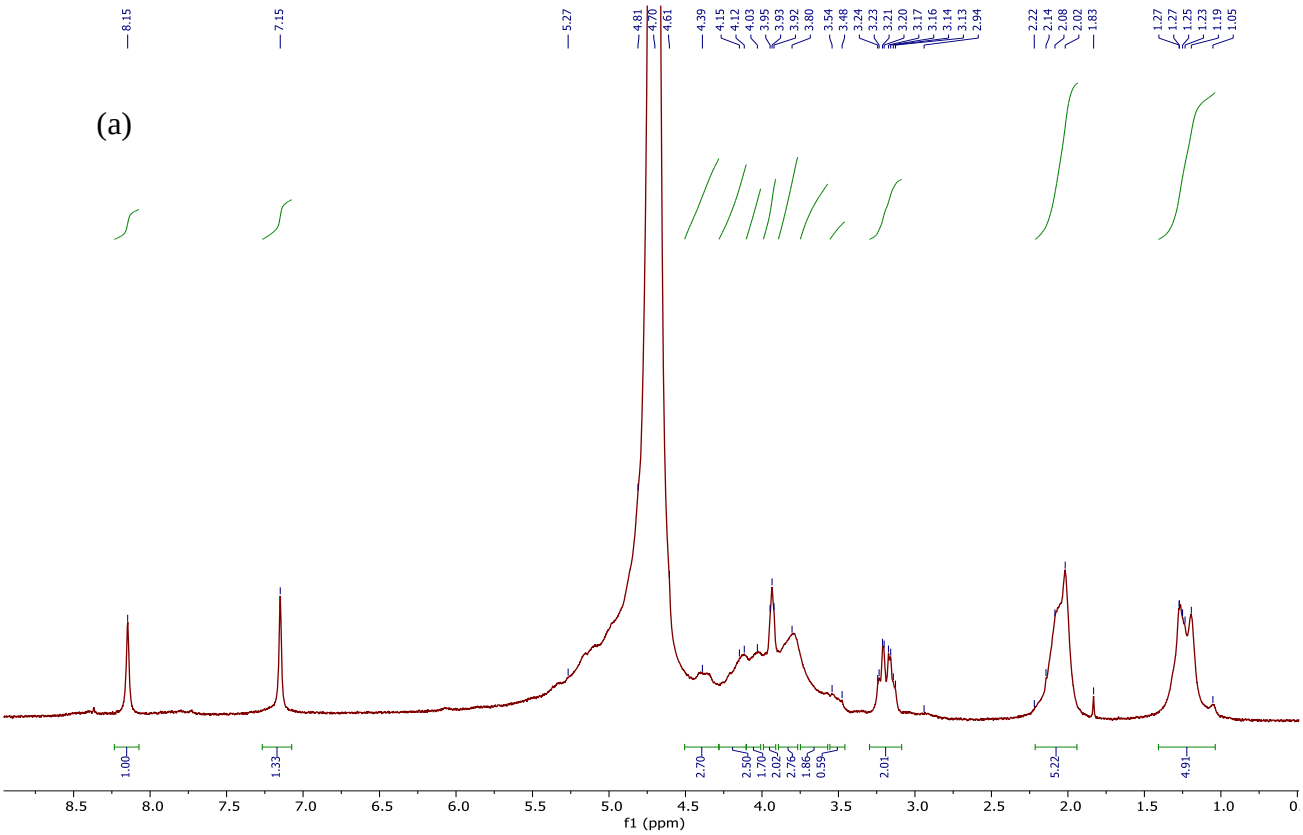
(a)
8.15
7.15
5.27
4.81
4.70
4.61
4.39
4.15
4.12
4.03
3.95
3.93
3.92
3.80
3.54
3.48
3.24
3.23
3.21
3.20
3.17
3.16
3.14
3.13
2.94
2.22
2.14
2.08
2.02
1.83
1.27
1.27
1.25
1.23
1.19
1.05
1.00
1.33
2.70
2.50
1.70
2.02
2.76
1.86
0.59
2.01
5.22
4.91
f1 (ppm)

128
129

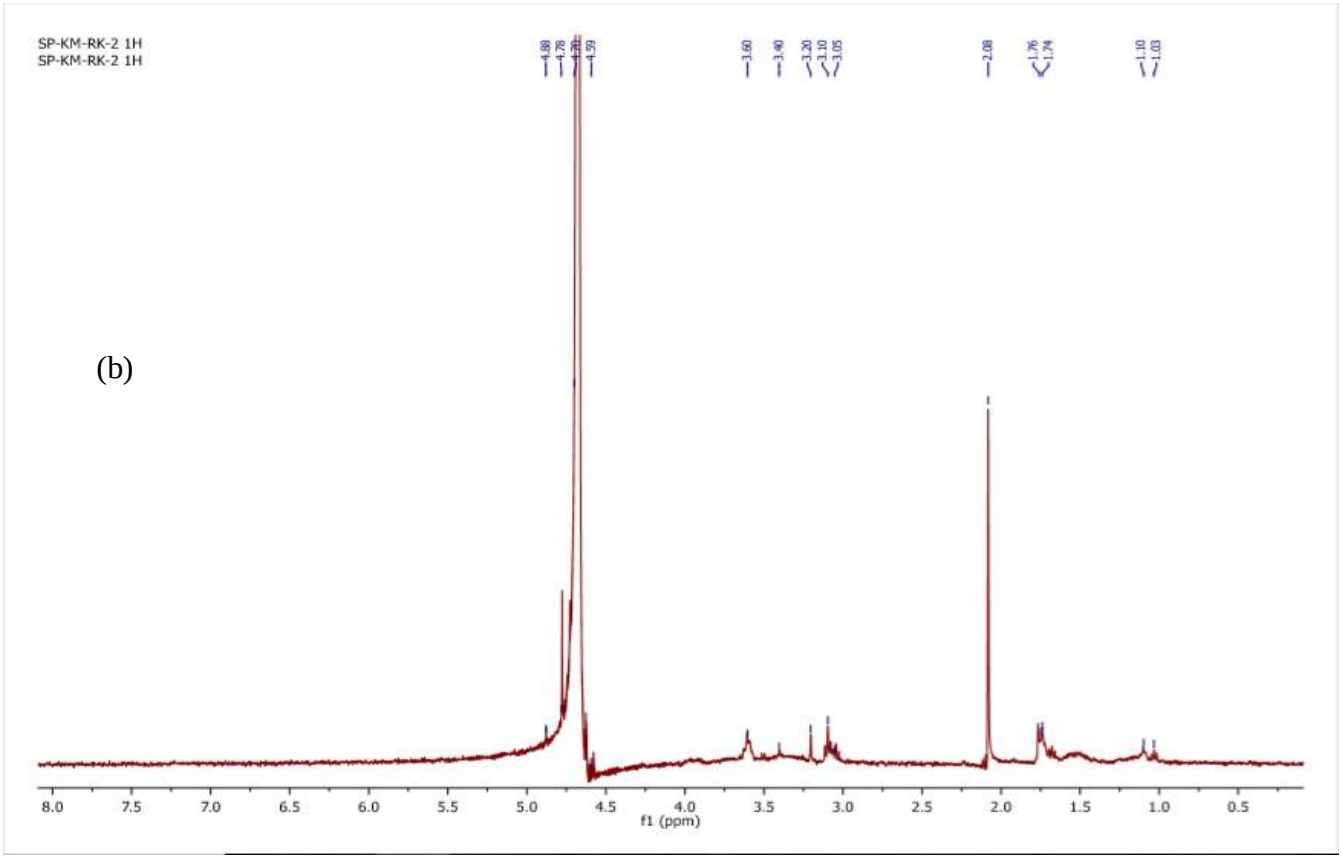
SP-KM-RK-2 1H
SP-KM-RK-2 1H
(b)
4.88
4.78
4.59
3.60
3.40
3.20
3.10
3.05
2.08
1.76
1.74
1.10
1.03
f1 (ppm)

130

Fig. S2 [1]HMR spectroscopy of (a) KGD (b) KGDR.

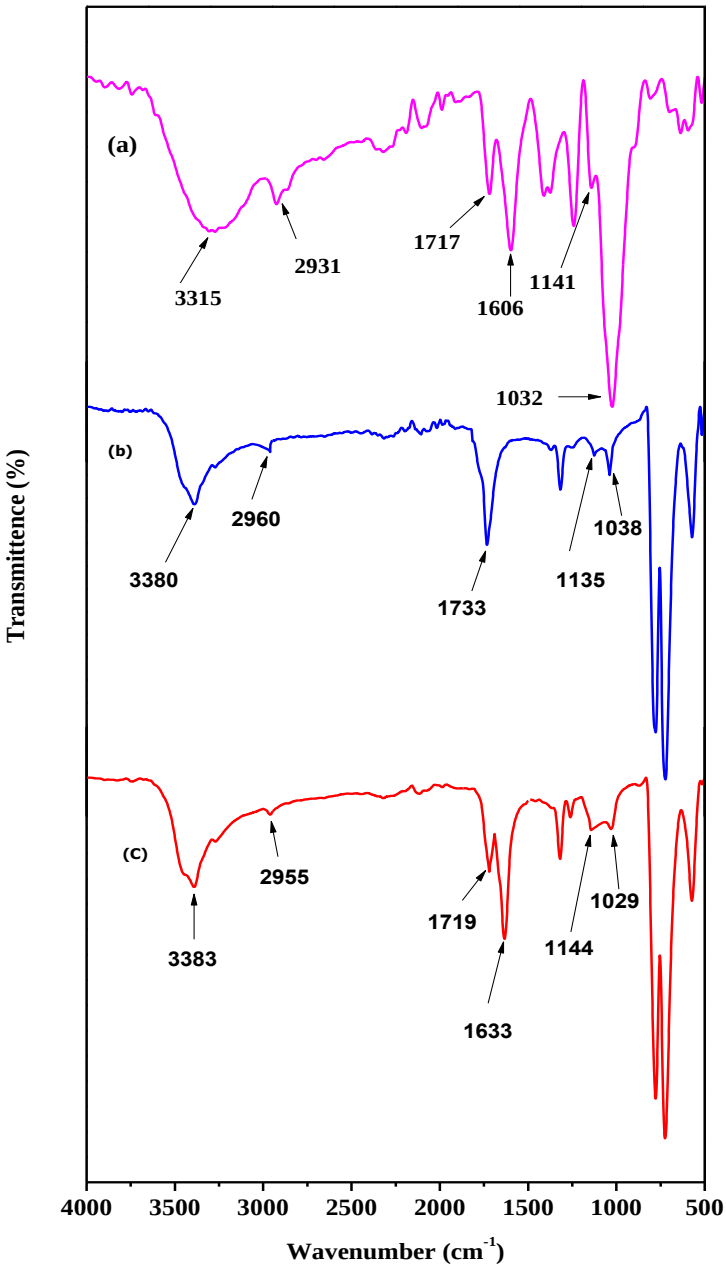

Fig. S3 FTIR spectra of (a) KG (b) KGD (c) KGDR

154

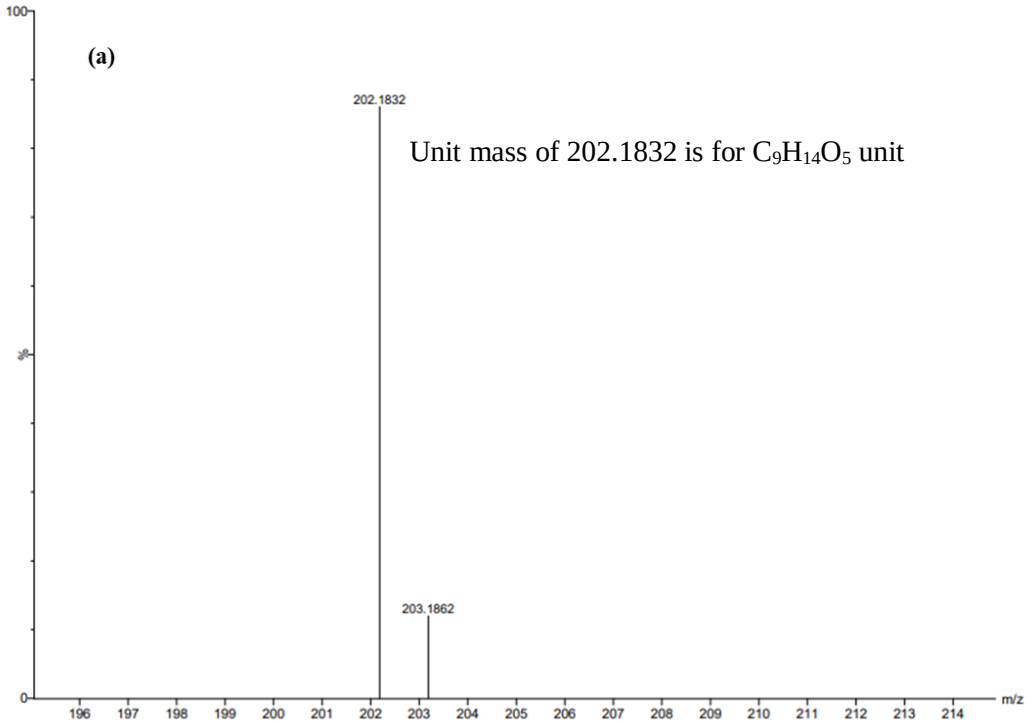
100
(a)
202.1832
Unit mass of 202.1832 is for $C_9H_{14}O_5$ unit
%
203.1862
0
196 197 198 199 200 201 202 203 204 205 206 207 208 209 210 211 212 213 214
m/z

155

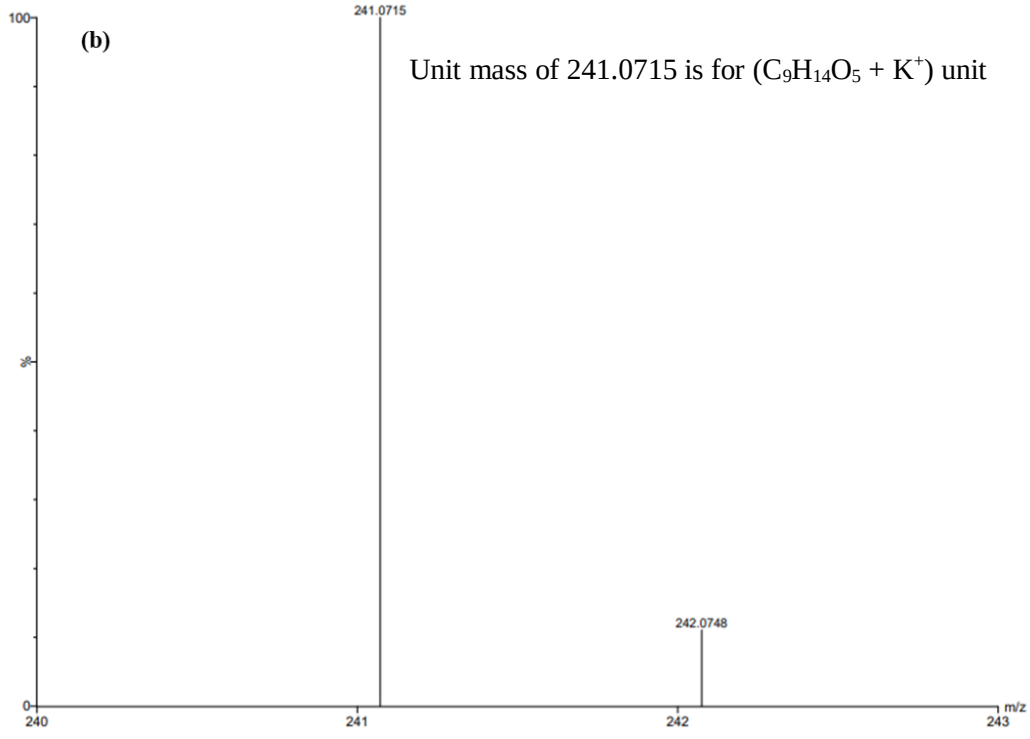
100
(b)
241.0715
Unit mass of 241.0715 is for ($C_9H_{14}O_5$ + K^+) unit
%
242.0748
0
240 241 242 243
m/z

156

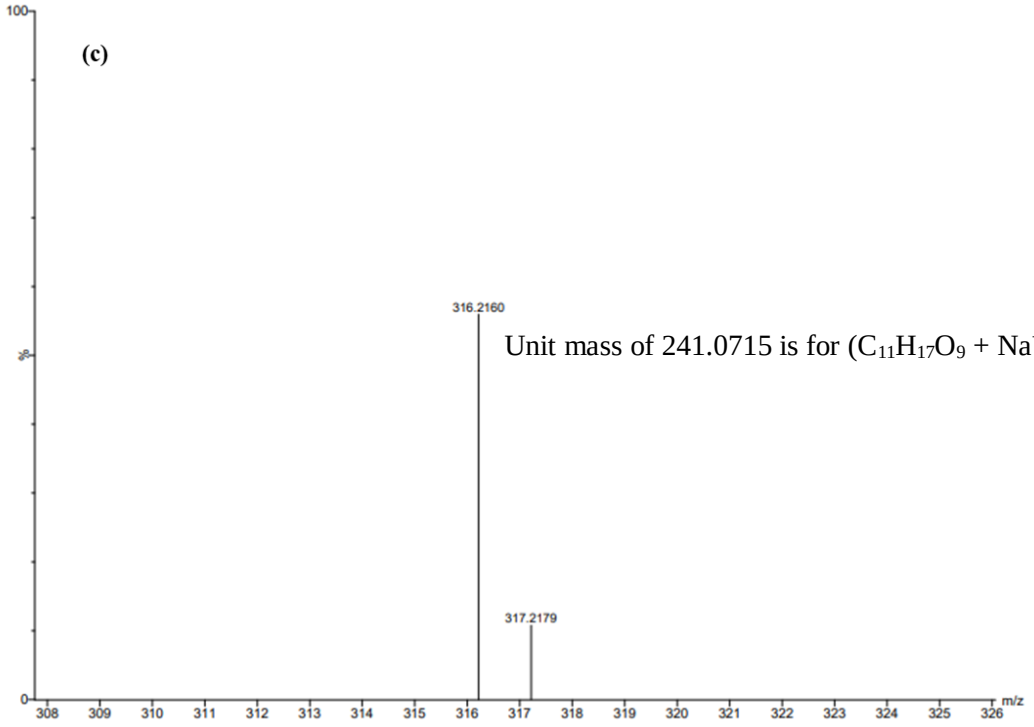

Unit mass of 241.0715 is for ($C_{11}H_{17}O_9 + Na^+$) unit

157

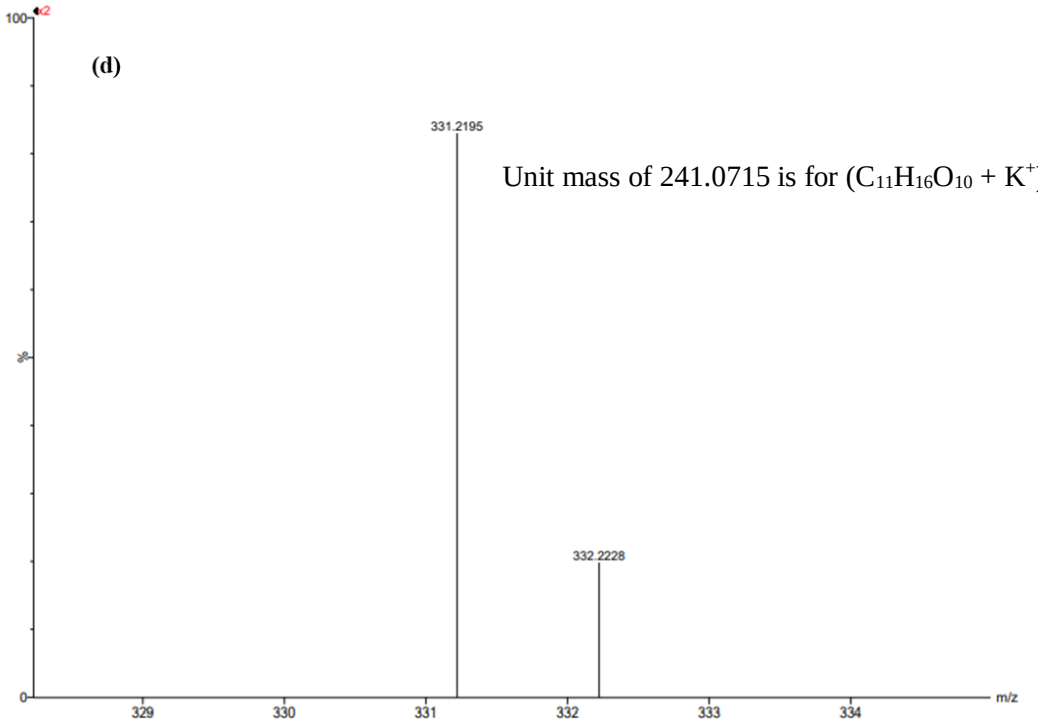

Unit mass of 241.0715 is for ($C_{11}H_{16}O_{10} + K^+$) unit

158

159

Fig. S4 High Resolution Mass Spectral analysis of KGD showed characteristic peaks for (a) $C_9H_{14}O_5$ molecular unit, (b) $C_9H_{14}O_5$molecular unit with K^+ cation, (c) $C_{11}H_{17}O_9$ molecular unit with Na^+ cation, and (d) $C_{11}H_{16}O_{10}$ molecular unit with K^+ cation.

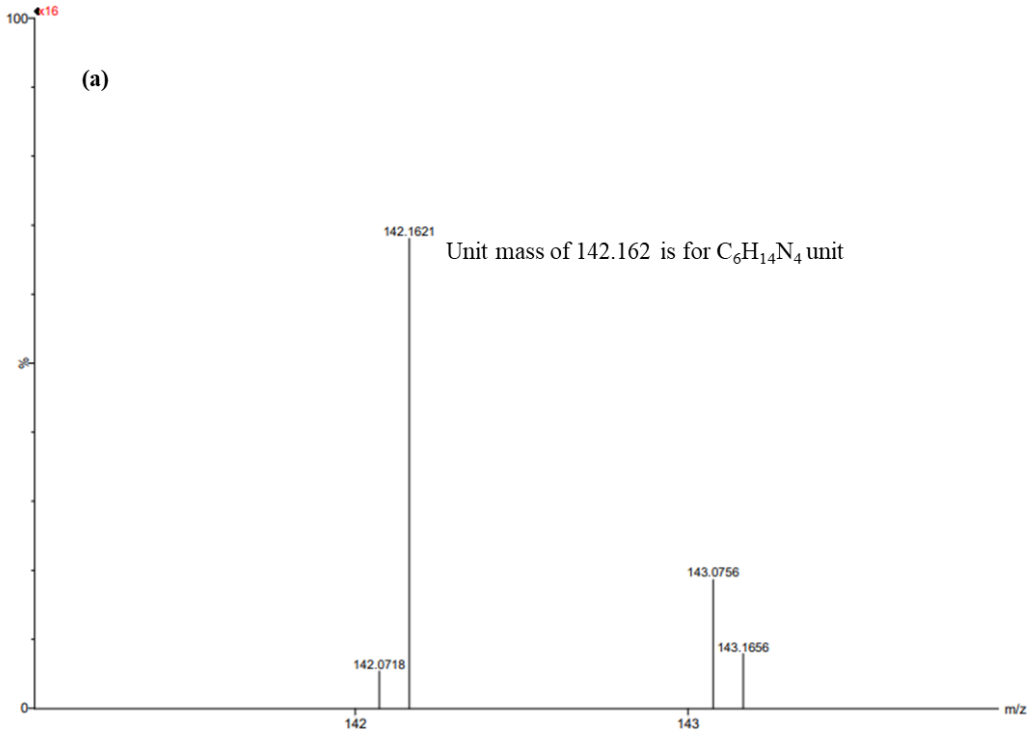

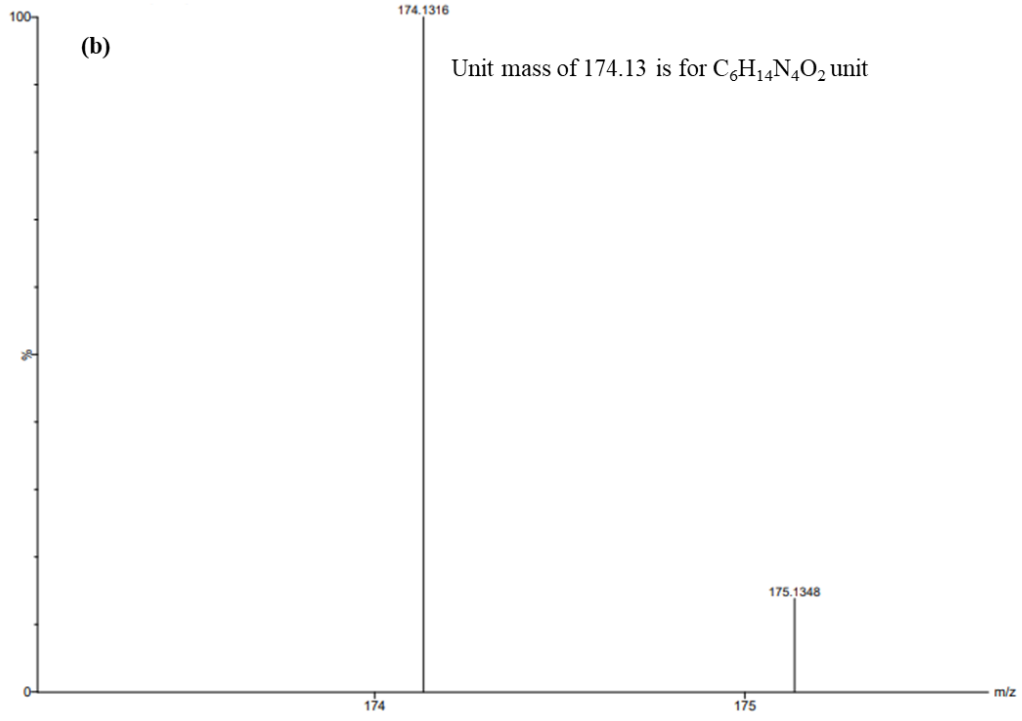

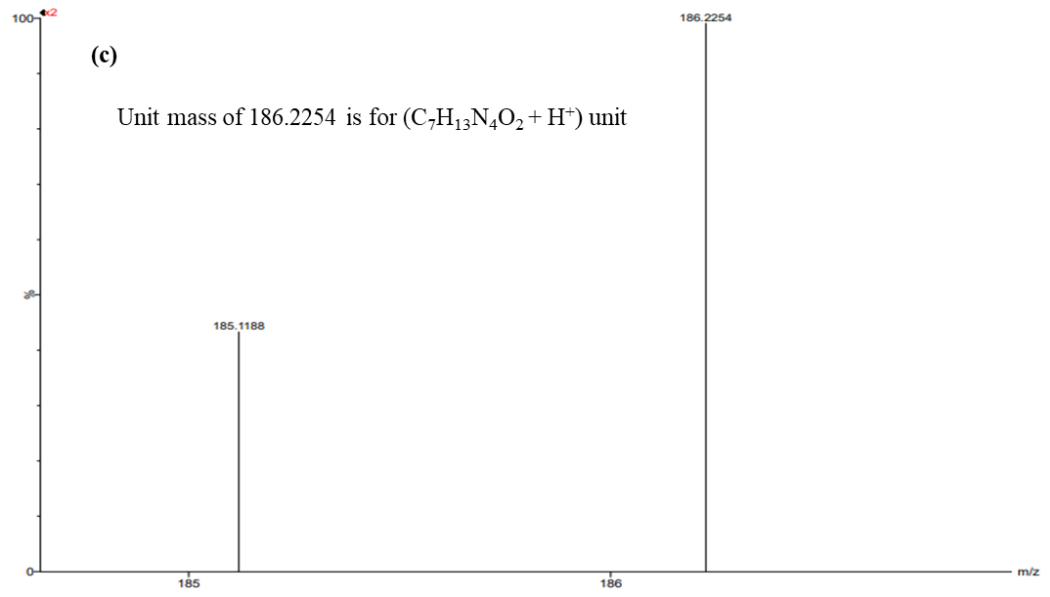

Fig. S5 High Resolution Mass Spectral analysis of KGDR showed characteristic peaks for (a) $C_6H_{14}N_4$ unit, (b) $C_6H_{14}N_4O_2$ unit, and (c) $C_7H_{13}N_4O_2$ unit with H^+ cation.

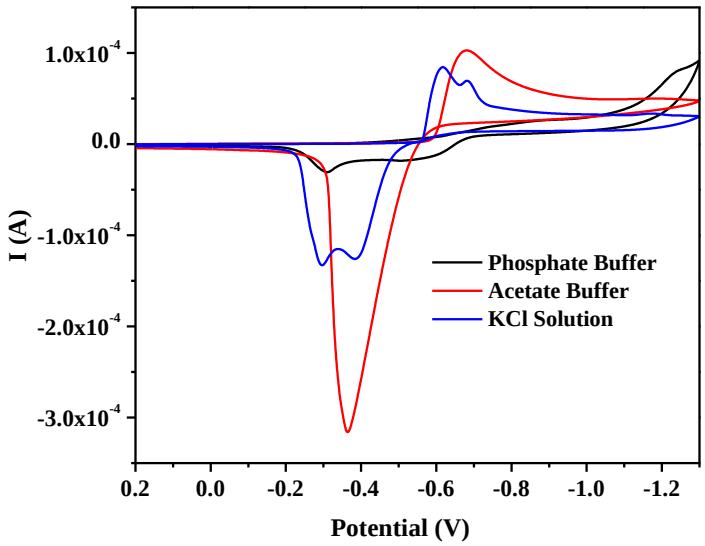

Fig. S6 CV analysis of KGDR/GCE in various electrolyte solutions (pH=5).

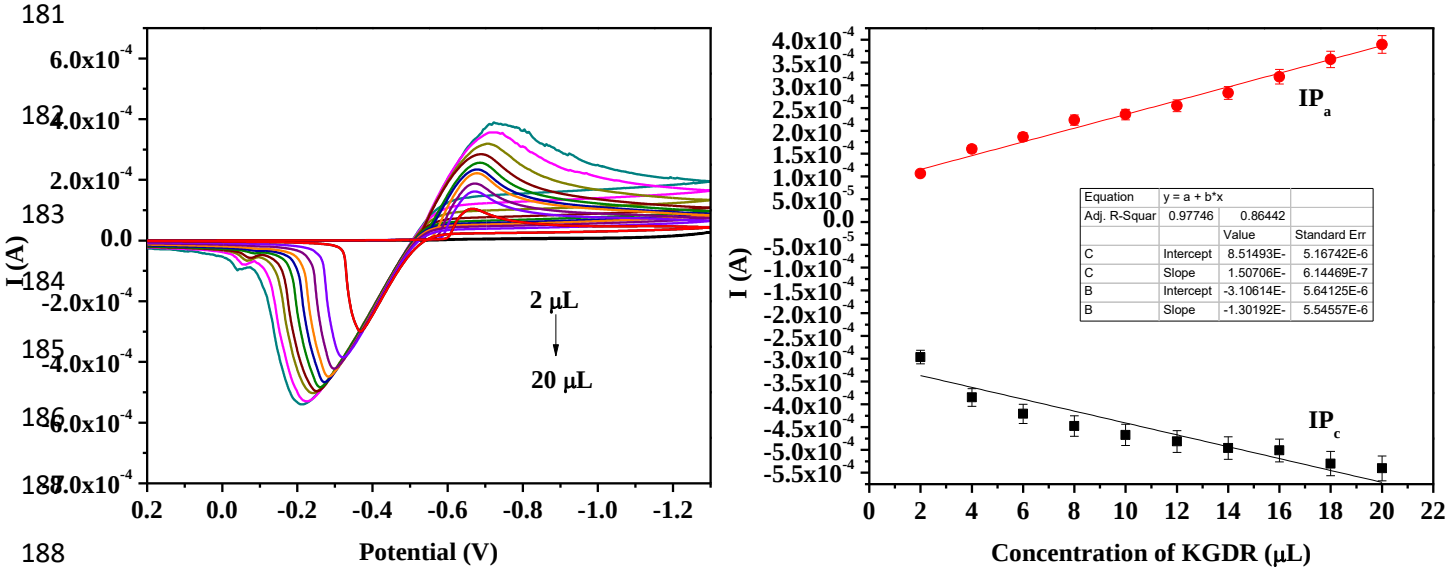

Fig. S7 (a) CV analysis of KGDR/GCE in 0.1 (M) ABS (pH 5) at various concentrations of KGDR (2µL to 20µL). (b) Calibration curve of peak current (I (A)) versus concentration of KGDR.

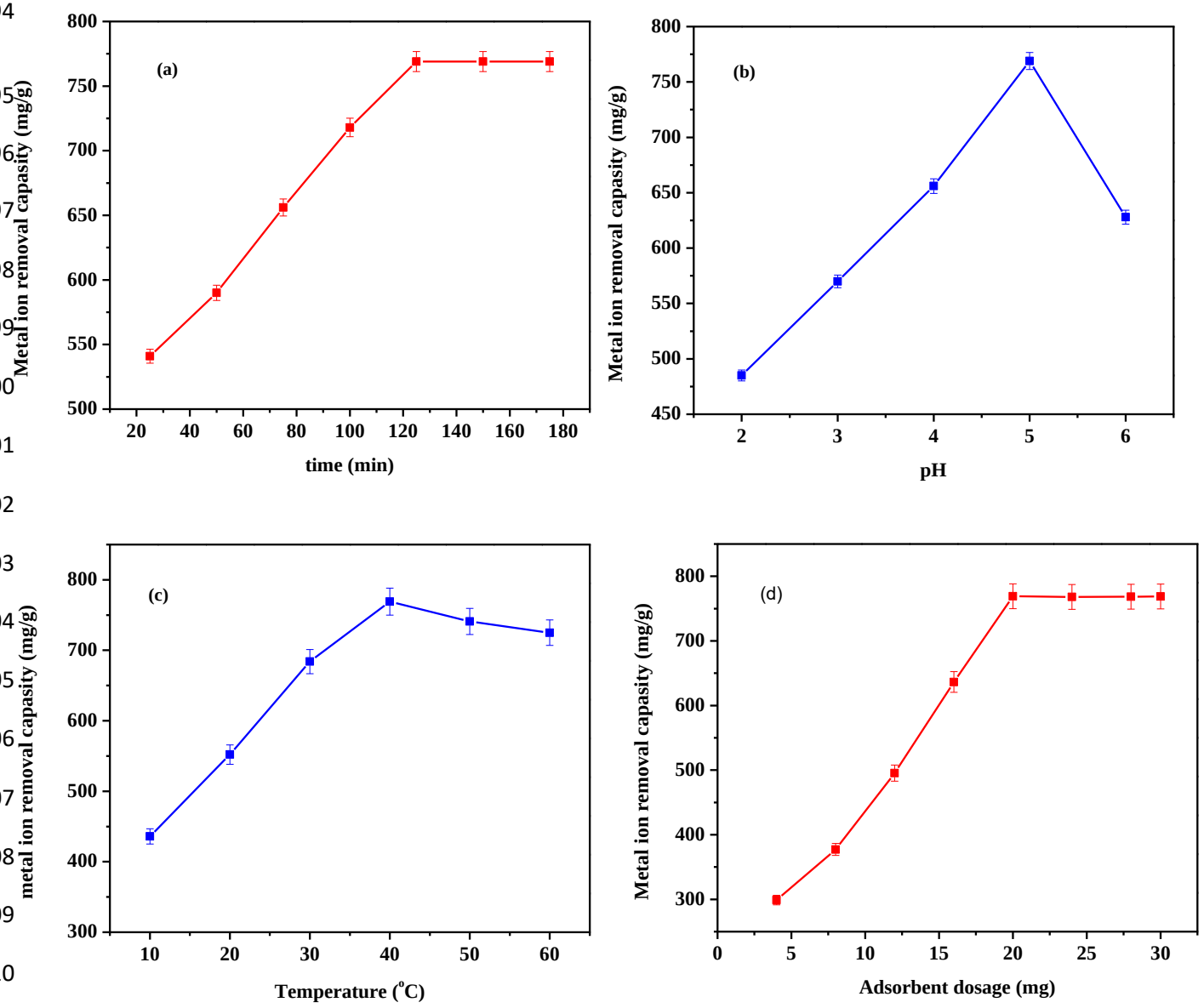

Fig. S8 Effect of (a) contact time (b) pH (c) temperature (d) adsorbent dosage of Pb^{2+} ion adsorption onto the surface of KGDR.

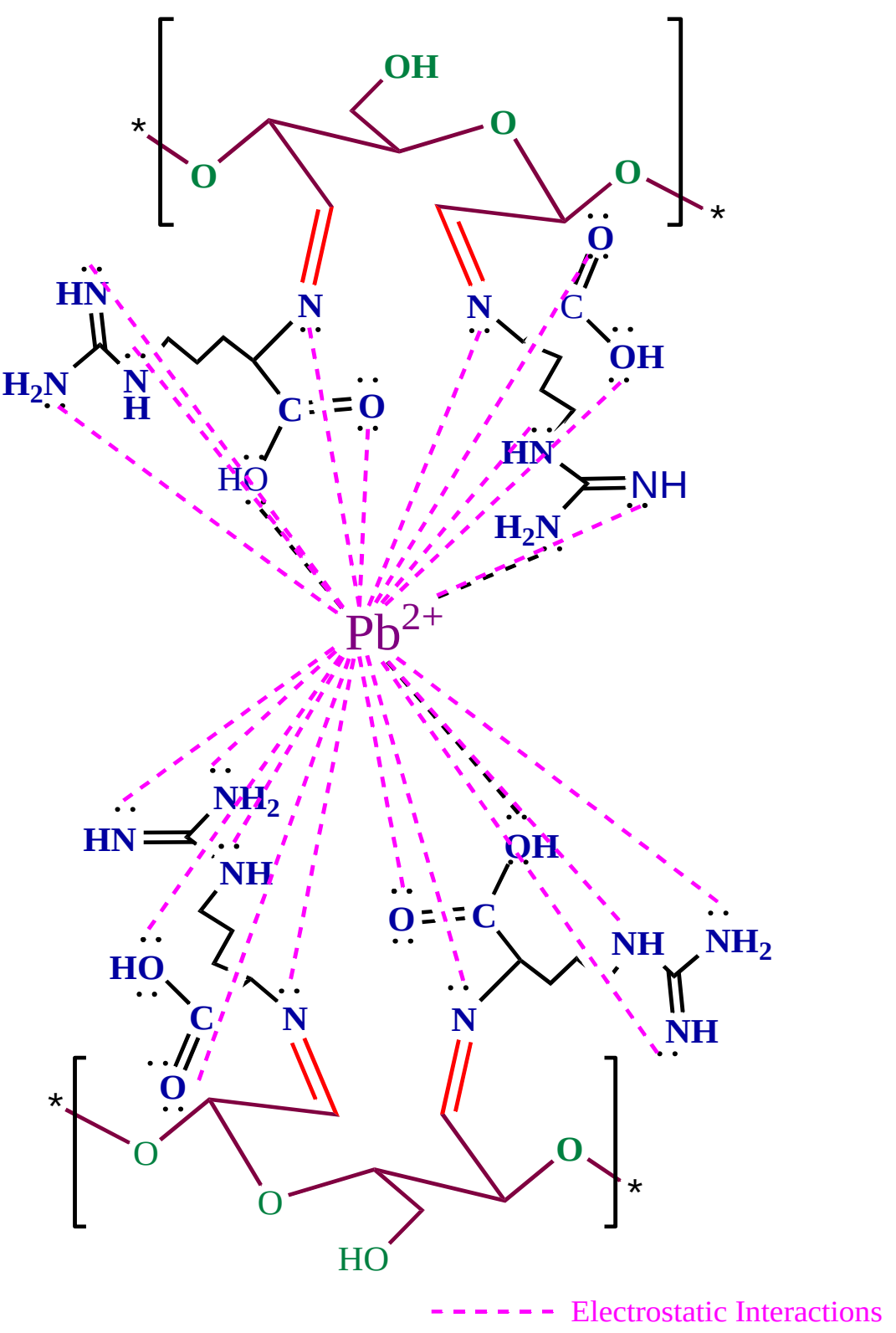

Fig. S9 Adsorption mechanism of KGDR.

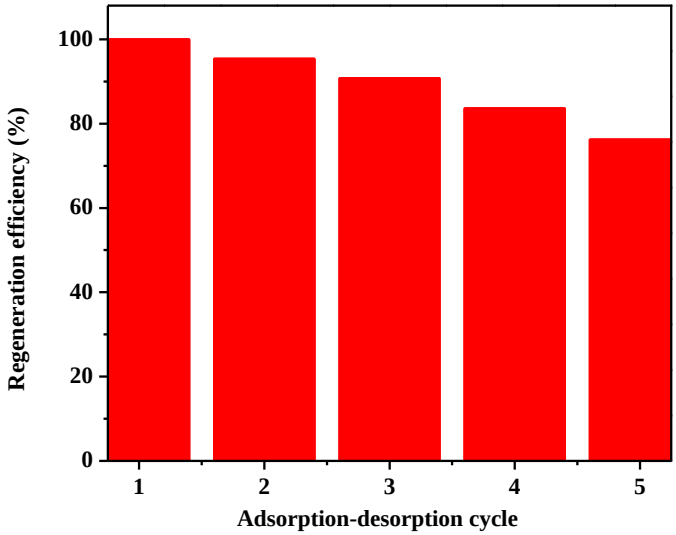

Fig. S10 Pb^{2+} ion adsorption-desorption cycle by KGDR.

Table S1 Comparison of KGDR/GCE with some previously reported works for sensing of Pb^{2+} ions.

Modifier	Method	Detection limit (µM)	Reference
CB-18-crown-6/GCE	DPASV	1.5	12
ZnFe2O4/GCE	DPASV	0.56	13
Salicylic acid	CV	0.18	14
P(DPA-co-2ABN)/GC-ME	DPASV	0.165	15
GSH-Fe3O4/GCE	SWASV	0.182	16
G/PANI/PS nanoporous fiber/GCE	CV	3.3	17
MWCNTs/synthesis Schiff base/CPE	SWASV	0.25	18
SWCNHs/SPE	SWASV	0.4	19
ZnO-Gr/SPCE	ASV	0.8	20
KGDR/GCE	CV	0.146	This work

DPASV: Differential pulse anodic stripping Voltammetry. CV: Cyclic Voltammetry

SWASV: square wave anodic stripping Voltammetry. ASV: anodic stripping Voltammetry

Table S2 Summary of the CV analysis of KGDR/GCE towards Pb^{2+} sensing from real samples.

Samples	Added Pb^{2+} ion (µM)	Obtained (µM)	Recovery %	RSD (%)
1	5	4.92	98.4	4.7
2	10	9.89	98.9	3.2
3	15	14.95	99.67	3.8

Table S3 Various parameters of adsorption kinetics along with their R^2 values for Pb^{2+} adsorption onto the surface of KGDR (Condition: Pb^{2+} ion concentration 1 g/L, 1.5 g/L, 2.07 g/L, 2.5 g/L, 3 g/L and 3.5 g/L, pH = 5, temperature 40˚C and contact time 125 min).

Pseudo-first-order-kinetics						
Concentration of Pb^{2+} ion (mg/L)	1000	1500	2070	2500	3000	3500
k_1 (min^{-1})	0.02012	0.01572	0.01836	0.02536	0.01828	0.02668
Standard Deviation (SD)	0.1096	0.01273	0.0986	0.2045	0.0109	0.1175
Co-relation Coefficient (R^2)	0.94513	0.88383	0.94662	0.88478	0.93958	0.96366
Pseudo-second-order-kinetics						
Concentration of Pb^{2+} ion (g/L)	1000	1500	2070	2500	3000	3500
k_2 (g/mg/min)	6.436×10^{-5}	4.866×10^{-5}	6.262×10^{-5}	1.202×10^{-5}	8.327×10^{-5}	3.948×10^{-5}
Standard Deviation (SD)	6.61×10^{-3}	8.52×10^{-3}	3.64×10^{-3}	1.55×10^{-3}	2.08×10^{-3}	2.47×10^{-4}
Co-relation Coefficient (R^2)	0.99290	0.98167	0.99535	0.99894	0.99725	0.99995
Intra particle diffusion						
Concentration of Pb^{2+} ion (g/L)	1000	1500	2070	2500	3000	3500
k_2 ($mg/g.min^{-1/2}$)	25.452	32.229	30.808	21.468	27.096	15.219
c (mg/g)	189.474	225.439	391.122	650.323	754.59	1135.772
Standard Deviation (SD)	16.324	20.542	18.149	15.348	15.961	18.388
Co-relation Coefficient (R^2)	0.93622	0.93697	0.94573	0.92175	0.94575	0.80065

Table S4 Various parameters of adsorption isotherms along with their R^2 values for Pb^{2+} adsorption onto the surface of KGDR (Condition: Pb^{2+} ion concentration 2.07 g/L, pH = 5, temperature 40˚C and contact time 125 min).

Langmuir Isotherm	
q_m ($mg.g^{-1}$)	5482.46
b ($L.mg^{-1}$)	5.985 x 10-5
R_L	0.8902
Standard Deviation (SD)	1.8896 x 10-5
Co-relation coefficient (R^2)	0.99746
Freundlich Isotherm	
K_F ($L.g^{-1}$)	0.00704
n	0.63
Standard Deviation (SD)	0.03302
Co-relation coefficient (R^2)	0.98709
Temkin Isotherm	
A_T ($L.g^{-1}$)	1.809
B ($J.mole^{-1}$)	0.00995
Standard Deviation (SD)	0.0351
Co-relation coefficient (R^2)	0.9629

Table S5 Various thermodynamic parameter for Pb^{2+} adsorption onto the surface of KGDR (Condition: Pb^{2+} ion concentration 2.07 g/L, pH = 5, temperature 20˚C to 60˚C and contact time 125 min).

Thermodynamic Parameters						
ΔH˚ (KJ/mole)			3.62			
ΔS˚ (J/K/mole)			14.384			
Temperature (K)	283	293	303	313	323	333
ΔG˚ (KJ/mole)	-0.45	-0.595	-0.738	-0.882	-1.026	-1.169

References

1. B. Gupta, M. Tummalapalli, B. L. Deopura and M. S. Alam, *Carbohydr. Polym.*, 2013, **98**, 1160-1165.

2. D. Sasmal, S. Banerjee, S. Senapati and T. Tripathy, *J. Environ. Chem. Eng.*, 2020, **8**, 103741.

3. B. Mondal, J. Ray, S. Jana, S. K. Bhanja and T. Tripathy, *New J. Chem.*, 2018, **42**, 19707-19719.

4. S. K. Lagergren, *Sven. Vetenskapsakad. Handingarl*, 1898, **24**, 1-39.

5. Y. S. Ho, *J. Hazard. Mater.*, 2006, **136**, 681-689.

6. W. J. Weber Jr and J. C. Morris, *J. Sanit. Eng. Div.*, 1963, **89**, 31-59.

7. H. Freundlich, *Z Phys Chem (N F)*, 1907, **57**, 385-470.

8. Y. S. Ho, C. T. Huang and H. W. Huang, *Process Biochem*, 2002, **37**, 1421-1430.

9. T. Karthikeyan, S. Rajgopal and L. R. Miranda, *J. Hazard. Mater.*, 2005, **124**, 192-199.

10. S. Jana, J. Ray, S. K. Bhanja and T. Tripathy, *J. Appl. Polym. Sci.*, 2018, **135**, 44849.

11. S. Jana, S. S. Pradhan and T. Tripathy, *J. Polym. Environ*., 2018, **26**, 2730-2747.

12. N. Serrano, A. González-Calabuig and M. Del Valle, *Talanta*, 2015, **138**, 130-137.

13. A. K. NS, S. Ashoka and P. Malingappa, *J. Environ. Chem. Eng.*, 2018, **6**, 6939-6946.

14. G. K. Raghu, S. Sampath and M. Pandurangappa, *J. Solid State Electrochem.*, 2012, **16**, 1953-1963.

15. M. F. Philips, A. I. Gopalan and K. P. Lee, 2012, *J. Hazard. Mater.* **237**, 46-54.

16. M. Baghayeri, A. Amiri, B. Maleki, Z. Alizadeh and O. Reiser, *Sens. Actuators B Chem.*, 2018, **273**, 1442-1450.

17. N. Promphet, P. Rattanarat, R. Rangkupan, O. Chailapakul, N. Rodthongkum, *Sens. Actuators B Chem.*, 2015, **207**, 526-534.

18. A. Afkhami, H. Ghaedi, T. Madrakian and M. Rezaeivala, *Electrochim. Acta*, 2013, **89**, 377-386.

19. Y. Yao, H. Wu and J. Ping, *Food Chem.*, 2019, **274**, 8-15.

20. J. Yukird, P. Kongsittikul, J. Qin, O. Chailapakul and N. Rodthongkum, *Synth. Met.*, 2018, **245**, 251-259.